Engineering and Technology Journal
Journal homepage: https://etj.uotechnology.edu.iq

Performance enhancement of PV panels by a channel shaped heat exchanger with an electromechanical control

Hussein A. Idan*, Hatam K. Kadhom, Sahar R. Faraj

Electromechanical Engineering Dept., University of Technology-Iraq, Alsina'a street, 10066 Baghdad, Iraq.
*Corresponding author Email: eme.20.02@grad.uotechnology.edu.iq

HIGHLIGHTS

- Effects of solar radiation and flow rate on new PVT design efficiency and output are investigated.
- A Finite volume analysis of the simulation model using ANSYS Fluent software is presented.
- A cooling system contributed to reducing the PV panel's average temperature.
- The control system affects the amount of water consumed.

ARTICLE INFO

Handling editor: Jalal M. Jalil

Keywords:
CFD; Control system; Photovoltaic panel; PV/T collector; Solar energy.

ABSTRACT

Photovoltaic panels are considered one of the important practical applications in converting solar energy into electrical energy, but they suffer from the effect of heat associated with solar radiation. Therefore, much research has been done to either harness the heat that comes with it or eliminate it by cooling the panel and boosting its effectiveness. In this work, a cooling box was designed and manufactured locally (the passage design is new) that is attached to the back wall as part of the panel without inserting an absorbent portion between it and the water to cool the panel. The new model was subjected to numerical and experimental tests to ascertain its efficacy in raising PV panel efficiency. ANSYS R19.2 software was used to compare numerical simulations with experimentally obtained results. The results showed good agreement between the two tests. The results also showed that the new model was able to raise the electrical efficiency of PV panels compared to the results of traditional panels without cooling, from 12.97% under the radiation intensity of 1035 W/m² to 14.87% under the same radiation intensity at a water flow rate of 4 L/min, this means an improvement of up to 12.78%. On the other hand, the control system reduced water consumption by 29.28% of the consumed water to maintain the efficiency ratio at semi-stable levels to its highest value of 15.37%, thus achieving an improvement of up to 15.56% for the same conditions above.

1. Introduction

The electrical energy produced by photovoltaic cells clearly indicates the use of solar energy to produce electrical energy. Still, it is greatly affected by the conversion efficiency, which is inversely proportional to the amount of heat associated with solar radiation. Therefore, a lot of research was conducted to find a technology that could take advantage of the radiation falling on the panel and the heat accompanying it, and the result was the PVT hybrid solar collector. The hybrid collector, or PVT, which generates electricity in addition to collecting heat using a thermal fluid (water or air) as the primary fluid that extracts the heat associated with radiation, is considered one of the most important methods that can be subject to further development and investment in solar energy compared to conventional photovoltaic panels and solar collectors are each separate, in terms of a better investment of space, resources, and costs [1].

In systems based on water use, there is a clear impact on the efficiency of the photovoltaic panel for different flow values by studying and analyzing the effect of a cooling system that uses water in channels and comparing it to another traditional panel without cooling [2,3]. Nanofluids and water were used with a small heat exchanger connected to channels mounted on the bottom wall of the photovoltaic panel to raise its performance, which has already improved [4]. Analytical and experimental results indicated that using V-shaped cooling channels or adding a heat sink to the back wall of the PV panel improves panel performance by increasing heat exchange surfaces and affecting fluid flow [5-7]. Numerical analysis was performed to show the effect of the size and number of ribs, ambient wind speed, and temperature, in addition to the velocity of the coolant entering the ribbed channel on the average cell temperature, and the results showed the high efficiency of this system [8].

http://doi.org/10.30684/etj.2024.143283.1575
Received 11 September 2023; Received in revised form 20 January 2024; Accepted 22 January 2024; Available online 18 February 2024
2412-0758/University of Technology-Iraq, Baghdad, Iraq

The type of fluid flow and its characteristics are of great importance in the heat transfer process. The characteristics of turbulent flow, as well as the effect of local heat transfer of a type of polygonal channel, were studied analytically within the boundaries of the turbulent region using the SST k-ω model for the case of turbulent flow within the limits of the Reynolds number 1800-3700. The analysis showed that the amount and extent of vortex pairs increase with increasing fin height (ribs) and that the fluid velocity near the bottom wall of the channel and the amount of resulting turbulence are the most important factors affecting heat exchange [9].

Many studies have been conducted on the modified photovoltaic module (PVT), which showed that its efficiency has reached good levels due to the dual use of electrical and thermal energy. On the other hand, using a water cooling system not only improves cell performance at a low cost but also provides reverse osmosis technology to cool water through preheating, which is more economical [10 -13]. Reviews also showed that passive cooling is less expensive and complicated than active cooling, which consumes part of the energy produced or external energy. In addition, reducing the average surface temperature of the PV panel is highly dependent on the coolant flow rate, as increasing it to optimum rates increases cell production and thus improves their efficiency. Cooling and cleaning the panel surface is also important [14 -16].

Although most previous studies worked to achieve ideal working conditions or those that increase the efficiency of photovoltaic panels, they are still within the limits that can be researched and developed. This research aims to contribute to the knowledge of the effect of adding a cross-finned cooling box as part of the photovoltaic panel parts without any additional heat-absorbing part between the back wall (Tedlar) and the water, that is, as a single unit. Water is used as a coolant due to its effectiveness and low cost, and it is also the base fluid for most other development additives. On the other hand, the research aims to determine the possibility of maintaining the panel's electrical efficiency at its highest levels through an electromechanical control system.

2. Experimental methodology

The experimental part is divided into two parts. The first includes using a new installation to cool the PV panel by relying on water cooling to increase the panel's efficiency in producing electrical power. The second part is to find an effective control system to maintain the highest efficiency obtained by controlling the flow as radiation changes during daylight hours.

2.1 Fabrication and installation of an experimental rig

The experimental work includes a study of increasing the output efficiency of photovoltaic panels, the characteristics of whose layers appear in Table 1. This is done by reducing their temperature and enhancing heat transfer for a heat exchanger made of aluminum as a single block mounted on a surface. Back wall as part of a cross-flow PV panel using rectangular fins. The installation process is carried out without a break between the water passing inside the exchanger and the back plate surface.

The practical part, designed and implemented locally, is an experimental model consisting of a traditional panel without cooling and another cooled using water through a cooling box whose dimensions and final shape are shown in Figures 1a and 1b. The effect of the fins of the heat exchanger on the heat transfer rate and the percentage of improvement in the electrical efficiency was studied compared to the conventional photovoltaic panel, i.e., without cooling, as shown in Figure 2. This study can also reveal the extent of compatibility between experimental and theoretical results in the case of using different working conditions, such as flow rate (0.3, 0.5, 1, 2, 3, and 4 L/min), radiation intensity (400, 600, 813 and 1035 W/m²) and the temperature of both the incoming water and the surrounding environment (air temperature) under stable working conditions.

Table 1: Characteristics of the Photovoltaic Panel Layers, [2,17]

Layer	Thickness (mm)	k (W/m. K)	ρ (kg/m³)	C_p (J/kg K)
Glass	3.0	1.0	3000	500
EVA	0.025	0.311	950	2090
Silicon Cells PV	0.30	148	2330	700
Tedlar	0.05	0.15	1200	1250

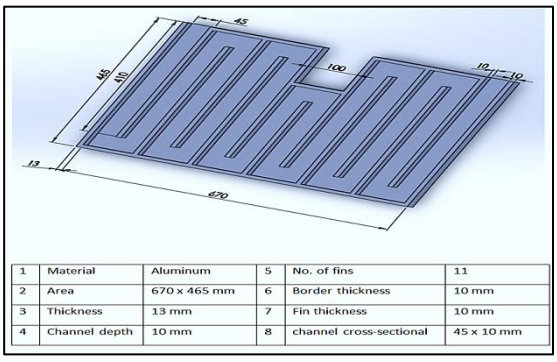

1	Material	Aluminum	5	No. of fins	11
2	Area	670 x 465 mm	6	Border thickness	10 mm
3	Thickness	13 mm	7	Fin thickness	10 mm
4	Channel depth	10 mm	8	channel cross-sectional	45 x 10 mm

(a)

(b)

Figure 1: (a) Schematic diagram of an aluminum cooler box with its dimensions, (b) Box manufacturing image

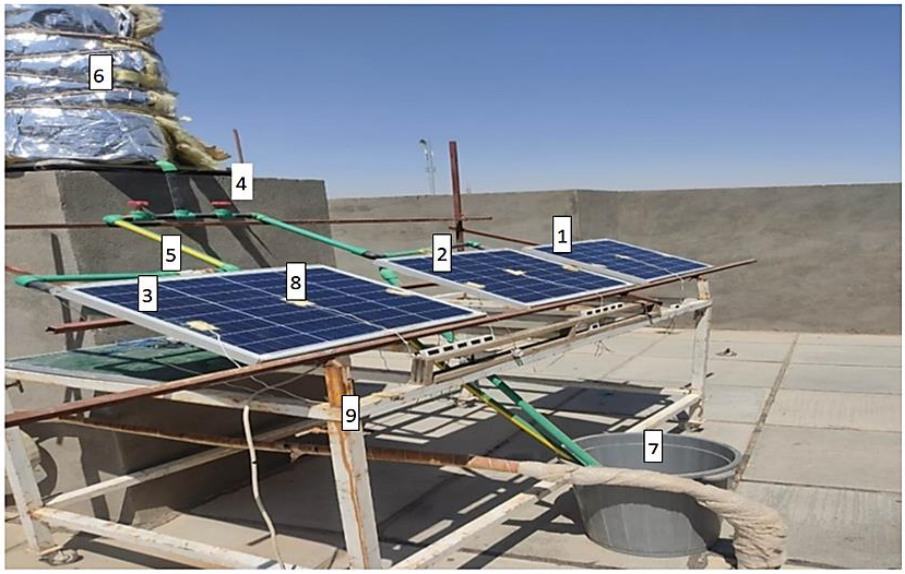

1	PV without cooling	6	Upper tank
2	PV with cooling without control system	7	Lower tank
3	PV with cooling with control system	8	Digital temperature sensors
4	Manual valve	9	Iron structure (rig)
5	Solenoid valve		

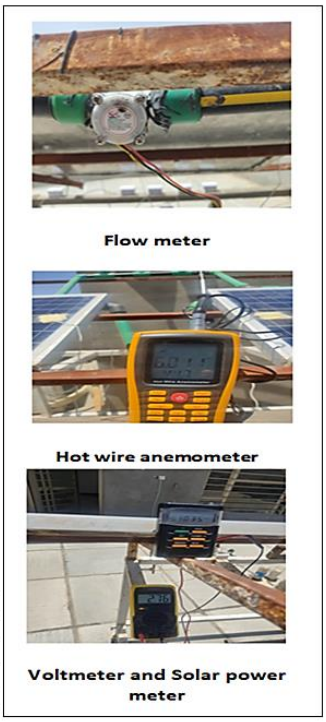

Figure 2: Photo of the experimental rig

2.2 Control system

Given that the electrical efficiency of photovoltaic panels is affected by changes in the intensity of solar radiation during daylight hours, it becomes important to find a way to maintain the efficiency at a constant or near-constant level. Through experimental and numerical tests, it was found that its efficiency depends mainly on the flow rate of cooling water in systems based on water cooling and the amount of solar radiation. However, the radiation intensity cannot be controlled during daylight hours because it is essential in operating photovoltaic panels. Therefore, this study determined the highest level required to maintain practically constant electrical efficiency: a flow rate of 7 L/min, as shown in Figure 3.

Allowing cooling water to flow at this rate from the early hours of the day, when there is not a significant difference between the temperature of the water used for cooling and the temperature of the surrounding air, until the noon hours when the difference is large, is necessary and constitutes a major waste of cooling water. On the other hand, monitoring temperature changes and manually changing the flow rate requires additional effort and costs. Therefore, an electromechanical control system was designed that relies on balancing the temperature of the water leaving the cooling box and the temperature of the water entering it through sensors and placing them at the outlet and inlet through a program to run the control circuit using an Arduino, whose parts and electrical connection circuit are shown in Figure 4a and 4b.

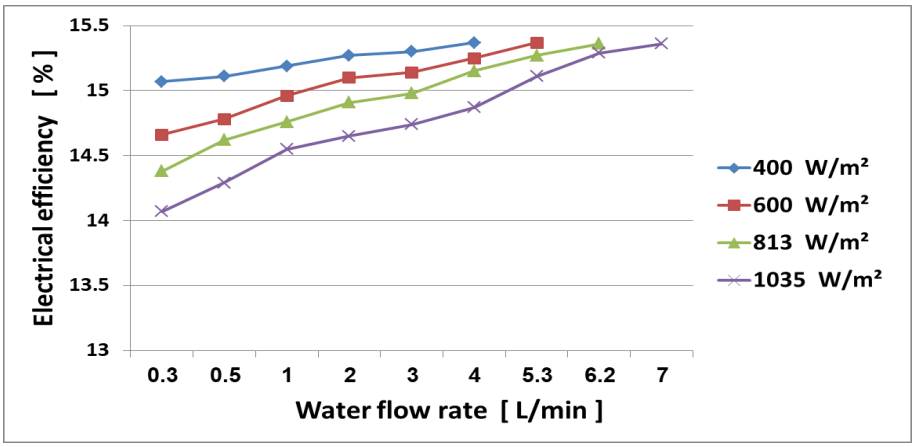

Figure 3: Effect of water flow rate on the performance of PV panel

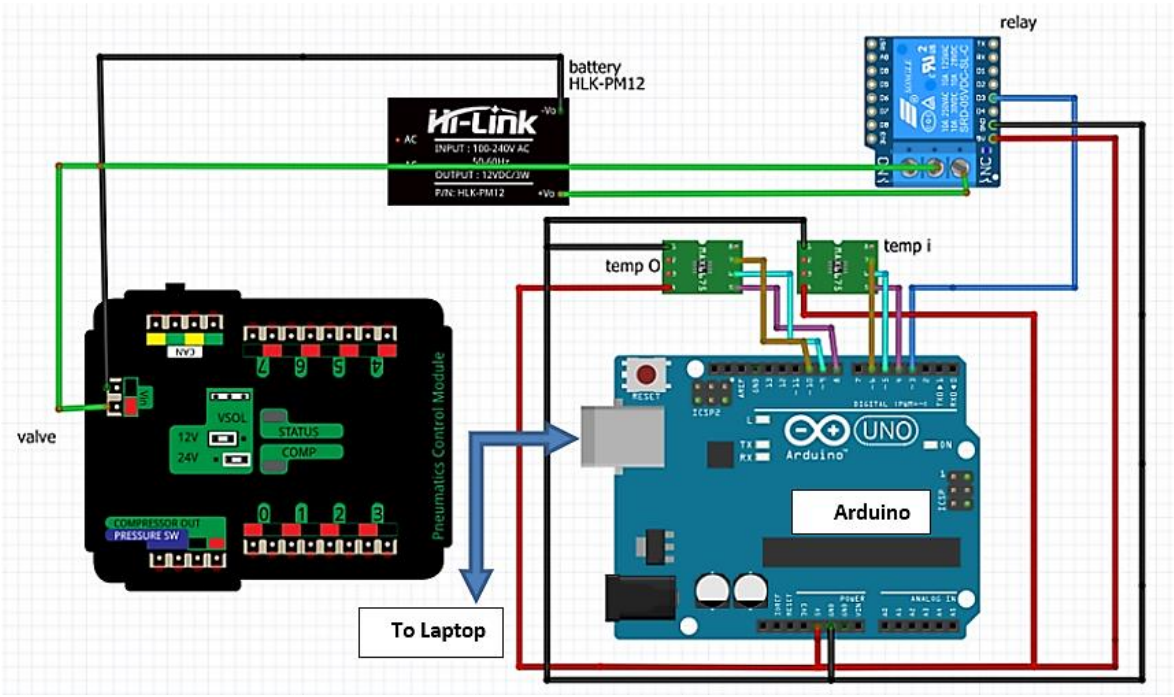

(a)

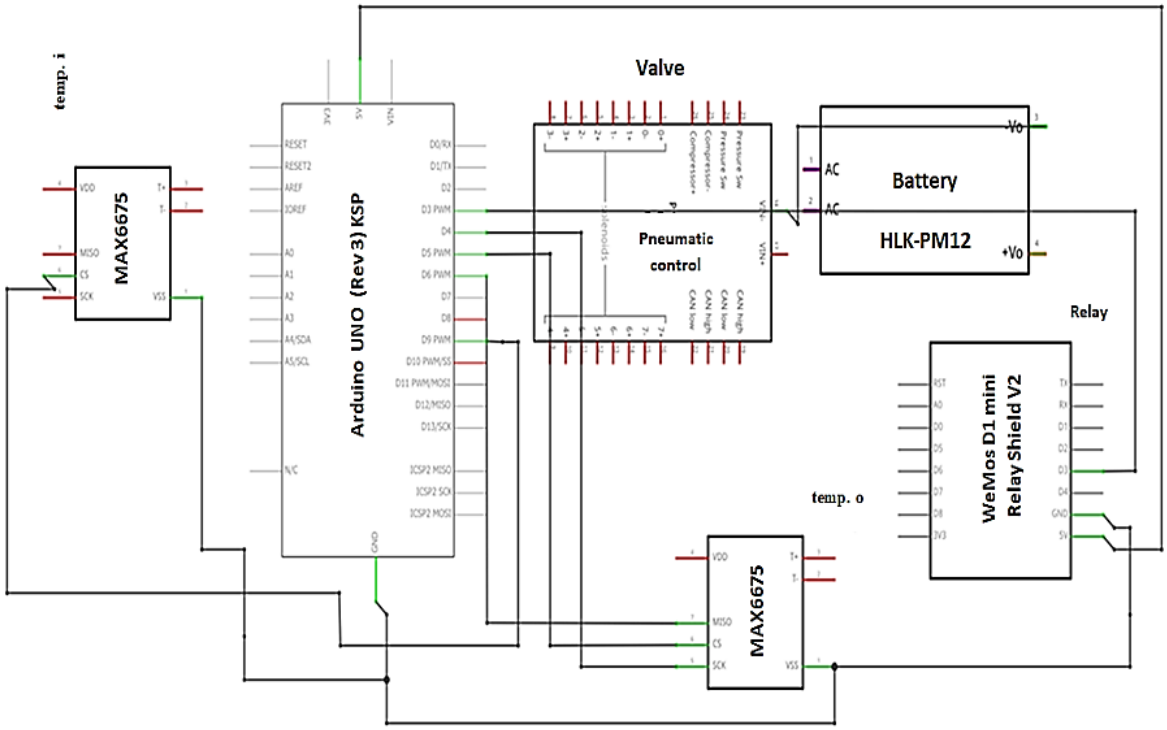

(b)

Figure 4: (a) Electrical control system (b) Electrical connection circuit

The program depends on the equation designed for calibration ($T_{water-out} - T_{water-in} <= 1$), through which the electric valve (Solenoid valve) is opened and closed, shown in Figure 5, which represents a picture of the experimental part of the operation of the control circuit.

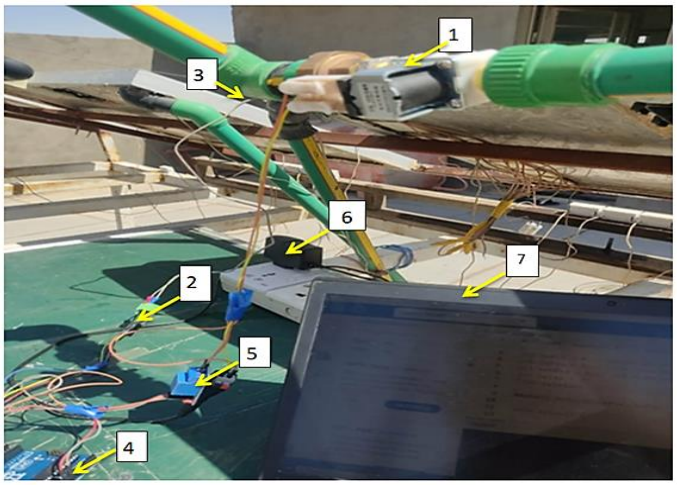

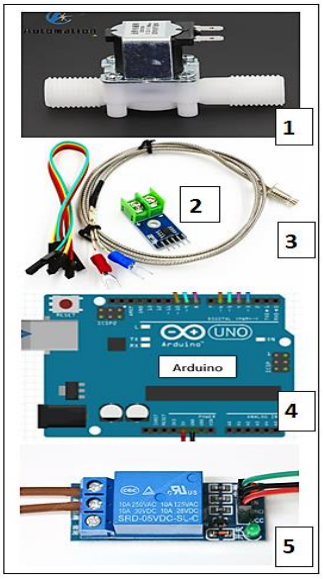

1	Solenoid Valve	5	Relay Module
2	MAX6675 Amplifier	6	12 volt Transf
3	K-Type Thermocouple	7	Laptop
4	Arduino (UNO)		

Figure 5: Experimental part of the operation of the control system

2.3 System's performance calculation

The importance of the tests lies in obtaining many conclusions from data extraction and comparing them to find out the competencies of the tested models or to evaluate the performance of a basic procedure or another attached to the tested system.

To practically calculate the power produced by PV panel, the general electrical power calculation law has been relied upon;

1) The output power of the PV panel is calculated by Equation (1) as follows ;

$$P_{output} = I_{measured} * V_{measured} \quad (1)$$

2) The electrical efficiency of the PV panel is calculated by Equation (2) as follows ;

$$\eta_{electrical\_PV} = P_{output} / P_{from\ radiation} = (I_{measured} * V_{measured}) / G.A_{panel} \quad (2)$$

where P_{output} It represents the output power at the measured current ($I_{measured}$) and measured voltage ($V_{measured}$). The intensity of solar radiation over the entire surface area of the panel (A_{panel}) is denoted by G.

3. Numerical simulation

This section examines the use of computational fluid dynamics (CFD) in simulating the water flow and temperature distribution of the PV panel surface and the water temperature at the outlet of the new PV/T cooling system. The simulation is done by entering data, including the water temperature at the inlet, the water flow rate, and the outside air temperature, in addition to the amount of solar radiation falling on the entire surface area of the panel, into the ANSYS software (version R19.2) after designing and drawing the model for the required condition using SOLIDWORKS explorer 2015.

3.1 Governing equations

The CFD model for solving 3D equations is most commonly used in software to predict what the temperature distribution will be like over the entire area of the PV panel and through the coolant, so here it is used to solve the Navier Stokes equations shown in Equations 3, 4, 5, 6, and 7 below;

3) Continuity Equation

$$\frac{\partial}{\partial x}(u) + \frac{\partial}{\partial y}(v) + \frac{\partial}{\partial z}(w) = 0 \quad (3)$$

4) Momentum Equation

$\vec{u}$-Momentum (in x- direction)

$$\frac{\partial(uu)}{\partial x} + \frac{\partial(vu)}{\partial y} + \frac{\partial(wu)}{\partial z} = -\frac{1}{\rho}.\frac{\partial p}{\partial x} + \frac{\mu}{\rho}\left(\frac{\partial^2 u}{\partial x^2} + \frac{\partial^2 u}{\partial y^2} + \frac{\partial^2 u}{\partial z^2}\right) \quad (4)$$

$\vec{v}$-Momentum (in y- direction)

$$\frac{\partial(uv)}{\partial x}+\frac{\partial(vv)}{\partial y}+\frac{\partial(wv)}{\partial z}=-\frac{1}{\rho}.\frac{\partial p}{\partial y}+\frac{\mu}{\rho}\left(\frac{\partial^2 v}{\partial x^2}+\frac{\partial^2 v}{\partial y^2}+\frac{\partial^2 v}{\partial z^2}\right) \quad (5)$$

$\vec{w}$-Momentum (in z-direction)

$$\frac{\partial(uw)}{\partial x}+\frac{\partial(vw)}{\partial y}+\frac{\partial(ww)}{\partial z}=-\frac{1}{\rho}.\frac{\partial p}{\partial z}+\frac{\mu}{\rho}\left(\frac{\partial^2 w}{\partial x^2}+\frac{\partial^2 w}{\partial y^2}+\frac{\partial^2 w}{\partial z^2}\right) \quad (6)$$

5) Energy Equation

$$\frac{\partial(uT)}{\partial x}+\frac{\partial(vT)}{\partial y}+\frac{\partial(wT)}{\partial z}=\frac{k}{\rho\, C_p}\left(\frac{\partial^2 T}{\partial x^2}+\frac{\partial^2 T}{\partial y^2}+\frac{\partial^2 T}{\partial z^2}\right) \quad (7)$$

where u, v, and w are the velocity (m/s) in x, y, and z direction, respectively, μ is the dynamic viscosity (kg/m. sec), k is the thermal conductivity (W/m. K), T is the temperature (K), ρ is the density (kg/m^3), and p is pressure measured in Pascal. To apply the above equations, some assumptions necessary to complete the solution must be taken into account, which are:

1) 3D steady-state incompressible.
2) 3D thermal conductivity through photovoltaic panels.
3) Use average temperature (T_{ave}) to find all properties of the working fluid.

3.2 Computing technique and operating conditions

The ANSYS and SOLIDWORKS programs are among the most widely used programs in drawing and analysis. The SOLIDWORKS Explorer 2015 program was used for drawing. Then, it was inserted into ANSYS FLUENT version R19.2 to perform laminar and turbulent flow simulations for the flows mentioned in the experimental part. In addition to cooling water, photovoltaic cells with all its parts were simulated. The model in the program consists of several nodes and elements for the liquid and solid parts, in addition to the communication elements, as it reaches 40,840 nodes and 27,540 elements for the liquid and 174,900 nodes and 86,110 elements for the solid parts, while the communication elements are 1,156,544. Figures 6a and 6b show the selected network shapes according to the data in Table 2. It shows how to choose the optimal network for the model with a regular shape.

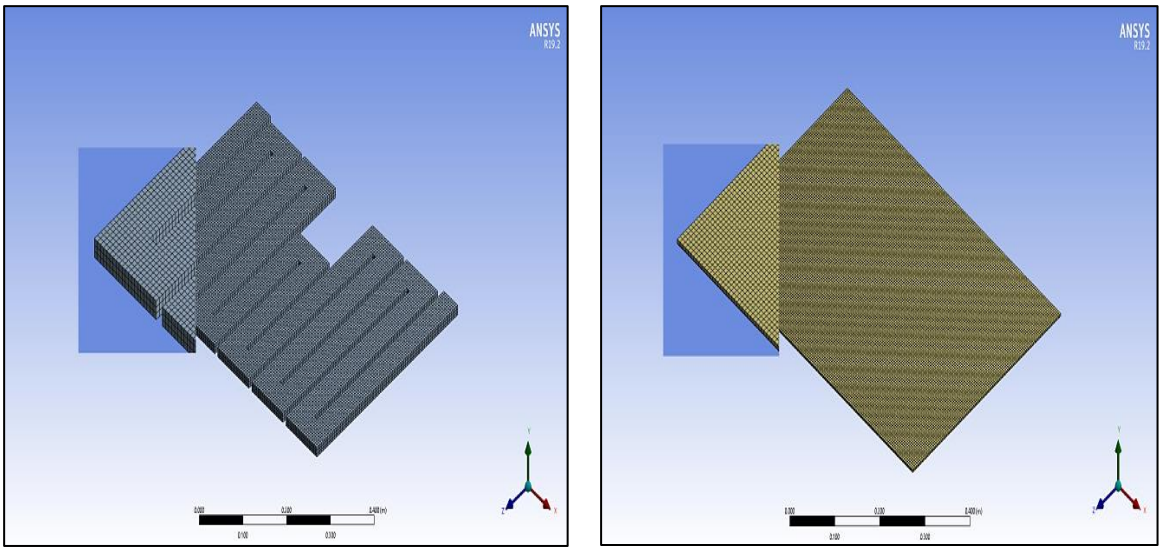

(a) **(b)**

Figure 6: Optimal mesh selected in ANSYS software for ; (a) Water inside the cooling box, and (b) PV panel

Determination of operating conditions is one of the most important factors for determining or analyzing the working environment. Therefore, the ambient and water temperatures at the cooler inlet were determined with the same experimental environment temperatures, water flow rates, and solar radiation mentioned in the experimental part. On the other hand, the properties of water are fixed, ρ = 998.2 Kg/m^3; (C_p) = 4182 J/kg-k. μ = 0.001003 (kg/m-s) and k = 0.6 W/m-k. The natural convection heat transfer coefficient on the photovoltaic components was calculated based on the wind speed in the experimental test environment. The comparison would be based on firm and practical foundations and accordance with Equation (8) shown below

$$h_a = 5.7 + 3.8\,(V_{wind}) \quad (8)$$

where h_a is the heat transfer coefficient between a glass PV panel and the surrounding air and V_{wind} is the wind velocity around the PV/T collector (m/s) [18].

Using the average temperature of the PV solar as a function of the Equation (9) below, the electrical efficiency of the photovoltaic panel can be obtained [3, 4, 8, 17, 19].

$$\eta_{electrical} = \eta_{ref}\ (1-0.0045(T_{pv(ave)} - 298)) \quad (9)$$

where η_{ref} is the efficiency of the PV module at the reference temperature and $T_{pv(ave)}$ represents the average PV temperature (K) [20,21].

To obtain the optimal solution for implementing the numerical simulation in the ANSYS Fluent software, the steps mentioned are followed in the flow chart shown in Figure 7, which further explains the sequence of the theoretical solution.

Table 2: Choosing the Optimum Mesh

Element size (mm)		**4.25**	**4.5**	**5.1**	**5.5**	**6.0**	**6.5**	**Optimum 4.25 +5.1**
Solar radiation (W/m²)		1000	1000	1000	1000	1000	1000	1000
PV panel	***Nodes***	174900	156000	121624	105780	89428	75920	174900
	Elements	86110	76735	59696	51850	43758	37080	86110
Element quality	***Min***	**0.01798**	0.0102	0.00898	0.00838	0.00769	0.007085	0.01798
(PV)	***Max***	**0.92856**	0.9058	0.08495	0.81556	0.77221	0.72992	0.92856
Water	***Nodes***	72965	50908	40840	34236	30248	18498	40840
	Elements	53416	34680	27540	22800	20037	10704	27540
Element quality	***Min***	0.96174	0.9923	**0.99925**	0.99056	0.76209	0.91224	0.99925
(Water)	***Max***	0.99248	0.9944	**1.0**	0.99346	0.99123	0.98862	1.0
Contact elements		1156544	103076	802294	696860	588384	498622	1156544
PV average temp.℃		37.572	36.540	36.389	36.468	36.444	37.55	36.368
Outlet water temp.℃		47.13	43.61	43.15	43.38	43.13	43.15	43.45

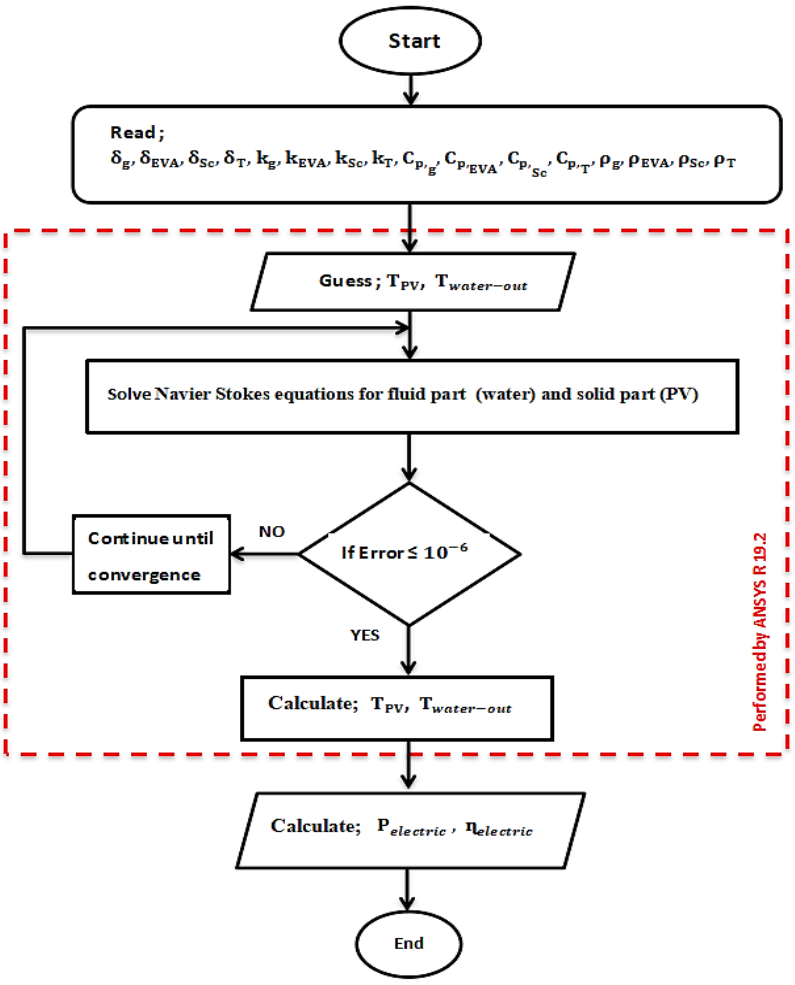

Figure 7: Flow chart of the numerical simulation

4. Results and discussion

This section presents the results of experimental and numerical tests conducted on three photovoltaic panels, one of which is a conventional reference one, and the other two contain a heat exchanger added to its back wall, one without a control system and the other with an electromechanical control system. A set of boundary conditions has been established to compare the panels' performance, and the effect of adding the heat exchanger (cooling box) and the control system is known.

4.1 Effect of inlet water flow rate on the PV panel average temperature

The average temperature of the PV panel in the new model generally drops as the water flow (Q) entering the cooler box increases, as illustrated in Figure 8a. The conventional panel temperature without cooling was 67.5 °C under a radiation flux of 1035 W/m², and it was reduced to 45.667 °C when the flow rate was as low as 0.3 L/min. In contrast, the high flow rate of 4 L/min achieved an additional decrease of 8.067 ℃ over the low flow rate. It should be noted that the PV panel's average temperature decreased to 37.267 °C and 33.167 ℃ at Q = 0.3 and 4 L/min, respectively, under a radiation rate of 400 W/m². While before this, the panel's temperature without cooling had been 44.4°C under the same radiation (400 W/m²).

Except for some temperature value differences that are smaller than those mentioned in the experimental part, Figure 8b illustrates how the variation of average PV panel temperature for the new model in the numerical part behaved by the behavior that is explained in detail in the analysis of the results of the experimental part above. The traditional panel recorded an average panel temperature of 65.532 °C at the highest radiation rate of 1035 W/m² and 45.247 °C at the lowest radiation intensity of 400 W/m². According to the new model, the average temperature of the PV panel reached its highest value of 43.926 °C under the radiation level of 1035 W/m² and Q = 0.3 L/min. Its lowest value was recorded at around 32.439 °C under the radiation level of 400 W/m² and Q = 4 L/min.

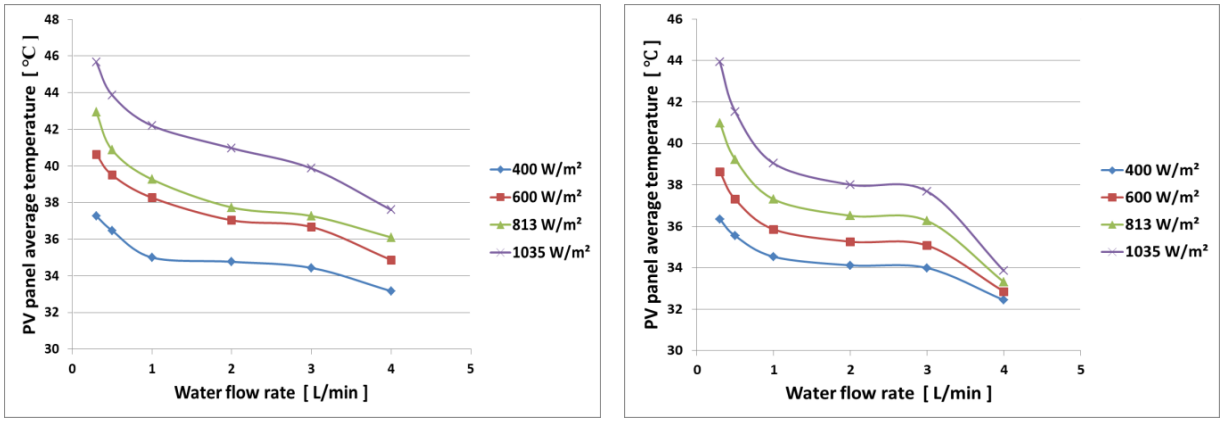

Figure 8: Effect of inlet feed water on PV panel average temperature for the value of different heat fluxes, (a) experimentally and (b) numerically

4.2 Effect of inlet water flow rate on the outlet water temperature

Since the outlet water temperature originates from heat transfer to the water entering the cooler box as a result of heat exchange between the back wall surface of the panel and water flowing through the box. Figure 9a illustrates how the outlet water temperature in the new model behaves similarly to the PV panel but slightly differently. The water temperature at the inlet is 31.5 °C. Under the radiation density level of 1035 W/m² rises to a maximum of 43.3 ℃ at Q = 0.3 L/min. However, as the flow rate increases, it decreases and reaches 33.7 ℃ at Q = 4 L/min, only 2.1°C above the inlet water temperature. Furthermore, it ought to be mentioned It should also be noted that the temperature of the outgoing water begins to decrease more than its previous rates when it was 2 and 3 L/min after the flow rate of 3 L/min, which is the transition zone from laminar flow to turbulent flow. The results shown in the graphs show that the lowest temperature of the outgoing water under a radiation level of 400 W/m² at Q = 4 L/min was 31.8 °C, a difference of 0.3 °C from the temperature of the incoming water after it was 35.5 ℃ at Q = 0.3 L/min. This behavior applies to the rest of the radiation levels, 600 and 813 W/m² with limited degrees between the two mentioned levels.

As for the numerical results, Figure 9b shows that the highest value was recorded under a radiation rate of 1035 W/m² at Q = 0.3 L/min at 46.98 °C, while the lowest value was recorded under a radiation rate of 400 W/m² at Q = 4 L/min where it reached 32.69 °C.

4.3 Effect of heat flux on PV panel average temperature

Figure 10a shows the effect of increasing the heat flux level on the average temperature of both the PV panel with cooler box and the conventional panel without cooling. It is evident from the figure that at the change in irradiation rate from 400 to 1035 W/m², the average temperature of the conventional panel and newly cooled model with a constant flow rate increase almost directly and linearly. The highest average temperature was recorded for the traditional panel under a radiation intensity of 1035 W/m², 67.5 ℃, while the lowest value was measured at a radiation intensity of 400 W/m², 44.4 ℃. As for the new

model, the average panel temperature's highest value was 45.667 ℃ at Q = 0.3 L/min. The lowest temperature was measured at the lowest level of fallout radiation on panel 400 W/m², as it was 33.167 ℃ for the average panel temperature of the new model, at Q =4 L/min.

As for the numerical test, Figure 10b shows that the highest average temperature of the conventional panel was under the radiation intensity of 1035 W/m², which amounted to 65.632 °C, while the lowest value was measured at the radiation intensity of 400 W/m², and it was 45.247 °C. As for the new model the highest average panel temperature value was measured at 43.926°C, at Q = 0.3 L/min. The lowest temperature was recorded at the lowest level of radiation falling on the panel 400 W/m² when it was 32.439 ℃ at Q = 4 L/min.

In addition to demonstrating the convergence of the experimental and numerical results at 11:55 am, when solar radiation is 1035 W/m² and for various flow rates, Figure 11 also displays similar behavior for both types of tests.

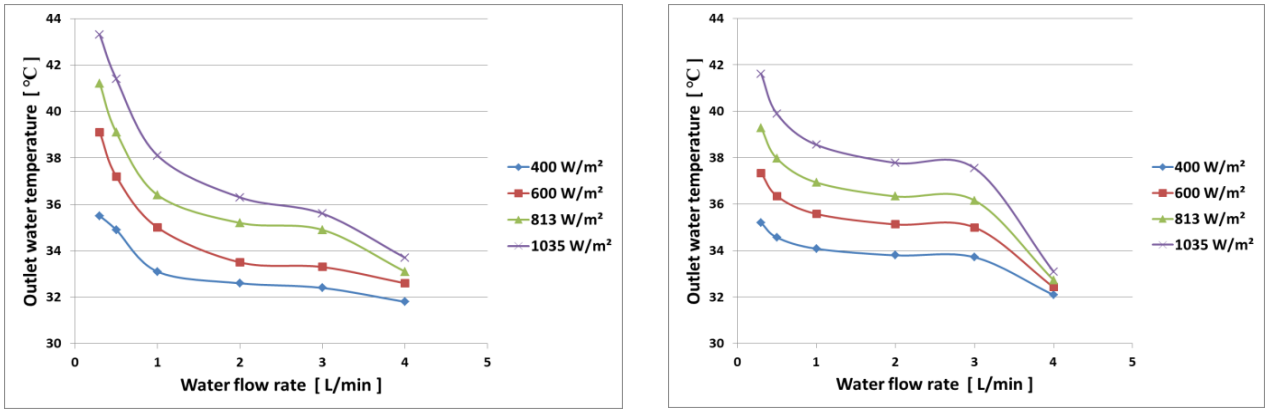

Figure 9: Effect of inlet feed water on the outlet water temperature for the value of different heat fluxes, (a) experimentally and (b) numerically

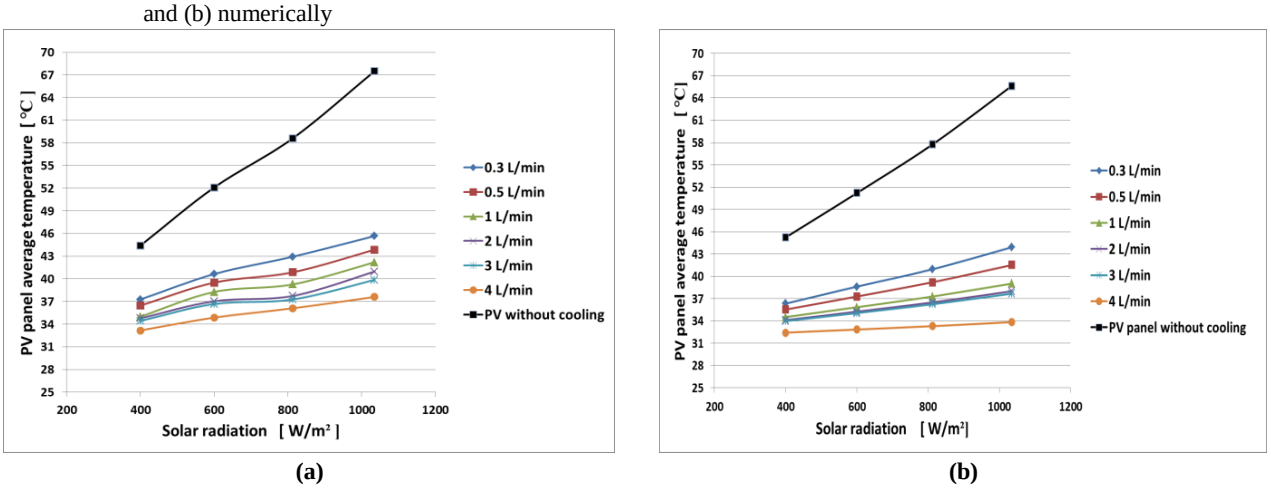

Figure 10: Effect of heat flux on PV panel average temperature for different values of water flow rates, (a) experimentally and (b) numerically

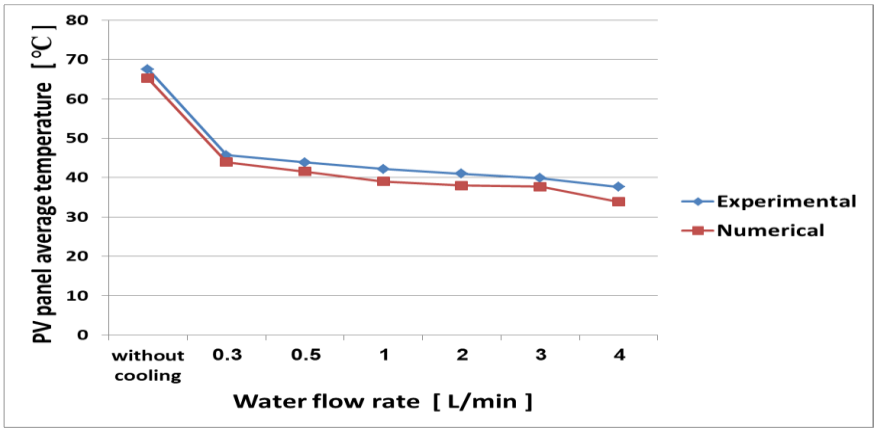

Figure 11: Effect of water flow rates on PV panel average temperature experimentally and numerically at 11:55 a.m, (solar radiation = 1035 W/m²)

4.4 Effect of heat flux on the outlet water temperature

Figure 12a shows the effect of increasing the level of heat flow on the temperature of the water leaving the heat exchanger, which takes the same behavior as the panel, as any increase in the temperature of the panel is transmitted to the water through the back wall (Tedlar) with which it is in direct contact. It is clear from the figure that when the radiation rate changes from 400 to 1035 W/m², the water temperature also increases directly and almost linearly. The highest temperature of the outlet water was recorded under the radiation intensity of 1035 W/m², which amounted to 43.3 ℃ at Q = 0.3 L/min, while the lowest value was measured at the radiation intensity of 400 W/m², which was 31.8 ℃ at Q = 4 L/min.

As for the numerical test, Figure 12b shows that the highest temperature of the water exiting the heat exchanger was under the radiation intensity of 1035 W/m², which amounted to 46.98 ℃, at Q = 0.3 L/min., while the lowest value was measured under the radiation intensity of 400 W/m², where it was 43.926 °C, at Q = 4 L/min.

4.5 Effect of changing flow rate and heat flux on electrical efficiency

Figure 13 shows the behavior of the photovoltaic panel by knowing the amount of change in its efficiency with increasing the flow rate for the water-cooled model and the traditional one without cooling and its behavior with increasing the intensity of solar radiation.

All curves show that the electrical efficiency increases with the increase in the cooling water flow under a constant radiation intensity. At the same time, it decreases with the increase in the radiation intensity when the flow rate is constant. The results showed that the cooled model significantly increased over the traditional panel. Its efficiency ranged from the highest value at a radiation density of 400 W/m², which reached 14.44%, and the lowest value at a radiation density of 1035 W/m², which was 12.97%. As for the cooled panel, it achieved an efficiency of 15.07%, 15.11%, 15.19%, 15.27%, 15.3%, and 15.37% at the radiation level of 400 W/m² for flow rates of 0.3, 0.5, 1, 2, 3 and 4 L/min, respectively. While the lowest value was achieved at the radiation intensity of 1035 W/m², it was 14.07%, 14.29%, 14.55%, 14.65%, 14.74%, and 14.87% at the same flow rates above.

The lowest improvement rate was recorded under the radiation rate of 400 W/m², where it reached 4.18% with a flow rate of 0.3 L/min, and this is normal because the radiation is at the beginning of the day and the cooling water temperature ($T_{inlet\ water}$) is close to the ambient air temperature, noting that panel performance under this radiation rate is at the highest value for all flow rates.

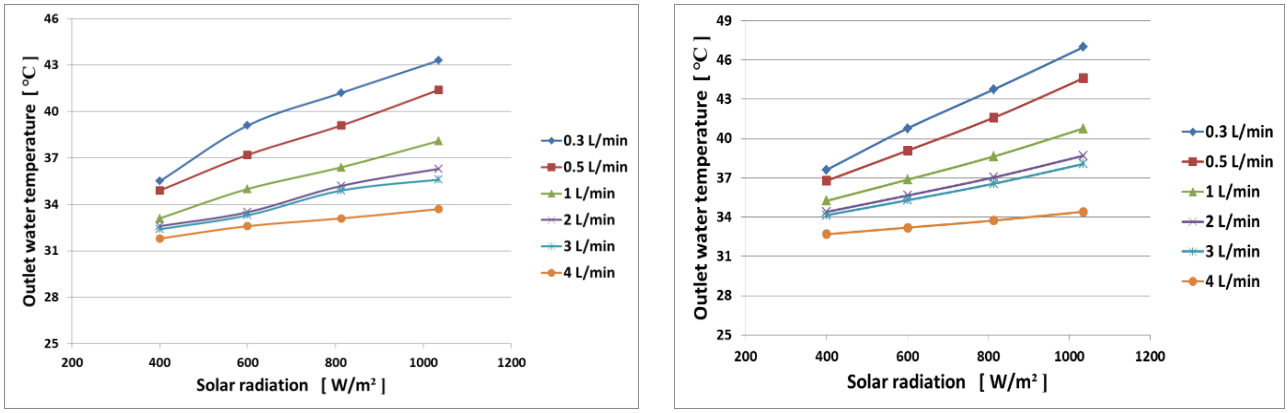

Figure 12: Effect of heat flux on the outlet water temperature for different values of water flow rates, (a) experimentally and (b) numerically

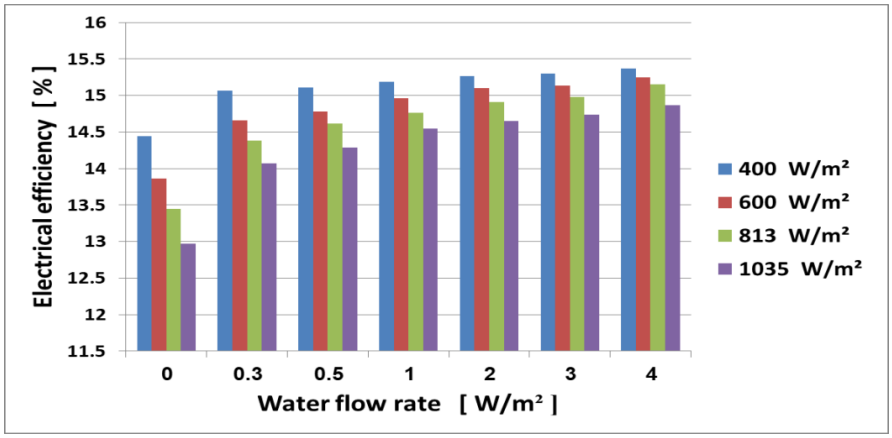

Figure 13: Change of electrical efficiency of a PV panel with increasing water flow rate in to its cooling box under different solar radiations (Experimental)

4.6 Effect of the control system

In the second part of the experimental test, the aforementioned control system was installed to control the flow rate during daylight hours to maintain electrical efficiency within its best value and reduce the effect of increased solar radiation.

Figure 14 shows how the electrical efficiency of the three panels changes under the same operating conditions. The effect of water cooling on the performance of the photovoltaic panel is very clear, as it raised the level of efficiency compared to the traditional panel without cooling to its highest value at a flow rate of 4 L/min and under a radiation rate of 400 W/m², reaching 15.37%. At the same time, its value for the traditional panel is 14.44%, which means an improvement of 6%. While the improvement rate increased to 12.78% at the radiation rate of 1035 W/m² for the same flow rate (4 L/min).

When observing the behavior of the cooled panel in the presence of a control system, its effect is evident in maintaining efficiency within semi-stable limits, raising the improvement rate to 15.56%, with its preference in reducing the consumption of cooling water, as shown in Table 3, where the rationalization of consumption reaches about 29.28% of the amount of water required to maintain efficiency at the same rate if the flow is left at 7 L/min.

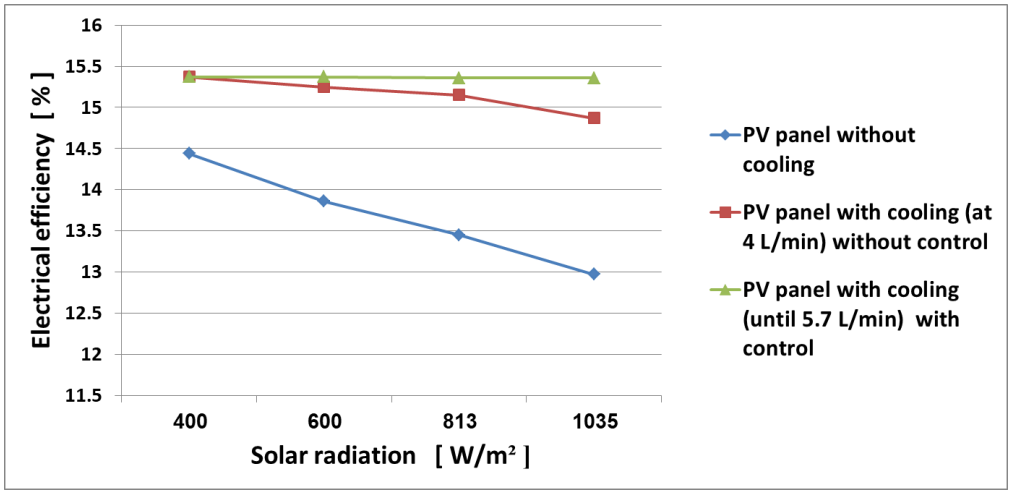

Figure 14: Comparison of the effect of the cooling system with and without the control system on the electrical efficiency

Table 3: Effect of Control System on PV Panel Performance

solar radiation W/m²	Air Temp. °C	Period of valve /ON min	Period of valve /OFFmin	Water flow rate L/min	Reduce water consumption L	$T_{PV\ panel}$ °C	$T_{water\ outlet}$ °C	$\eta_{electrical}$ %
400	35.2	22	18	4.0	126	33.167	31.8	15.37
600	38.1	35	22	4.3	154	33.333	32.1	15.369
813	40.0	57	20	5.2	140	33.40	32.3	15.364
1035	43.1	72	17	5.7	119	33.567	32.4	15.363

4.7 Temperature distribution over the entire photovoltaic panel

Figure 15 (a-f) shows the temperature distribution of the conventional and cooled panels. For the traditional panel, the temperature distribution takes a single pattern under the radiation intensity of 1035 W/m² and the rest of the other radiation densities, except for the edges that differ slightly due to heat exchange with the surrounding air currents. As for the cooled panel, when focusing on its contour charts, it is clear that the temperature distribution takes about six levels on the panel's surface when the water flows at a rate equal to 0.3 and 0.5 L/min. Temperatures are distributed irregularly on the panel's surface near the cooling box entrance. Still, they begin to coalesce as they approach the middle of the panel. In all cases, they are less regular than the area near the box outlet, which is more regular, as it represents the area corresponding to the part where the heat collects from hot water near the outlet. At flow rates of 1 to 3 L/min, the distribution levels start to become more uniform, forming 5, 4, and 3 levels at flow rates of 1, 2, and 3 L/min, respectively, but are less uniform at a flow rate of 4 L/min due to the appearance of hot spots at the edges and corners. This is normal for the flow speed, which creates a path for the flow away from corners and edges, and this, in turn, creates stagnant areas for the movement of the fluid, which affects the areas of the panel that come into contact with it.

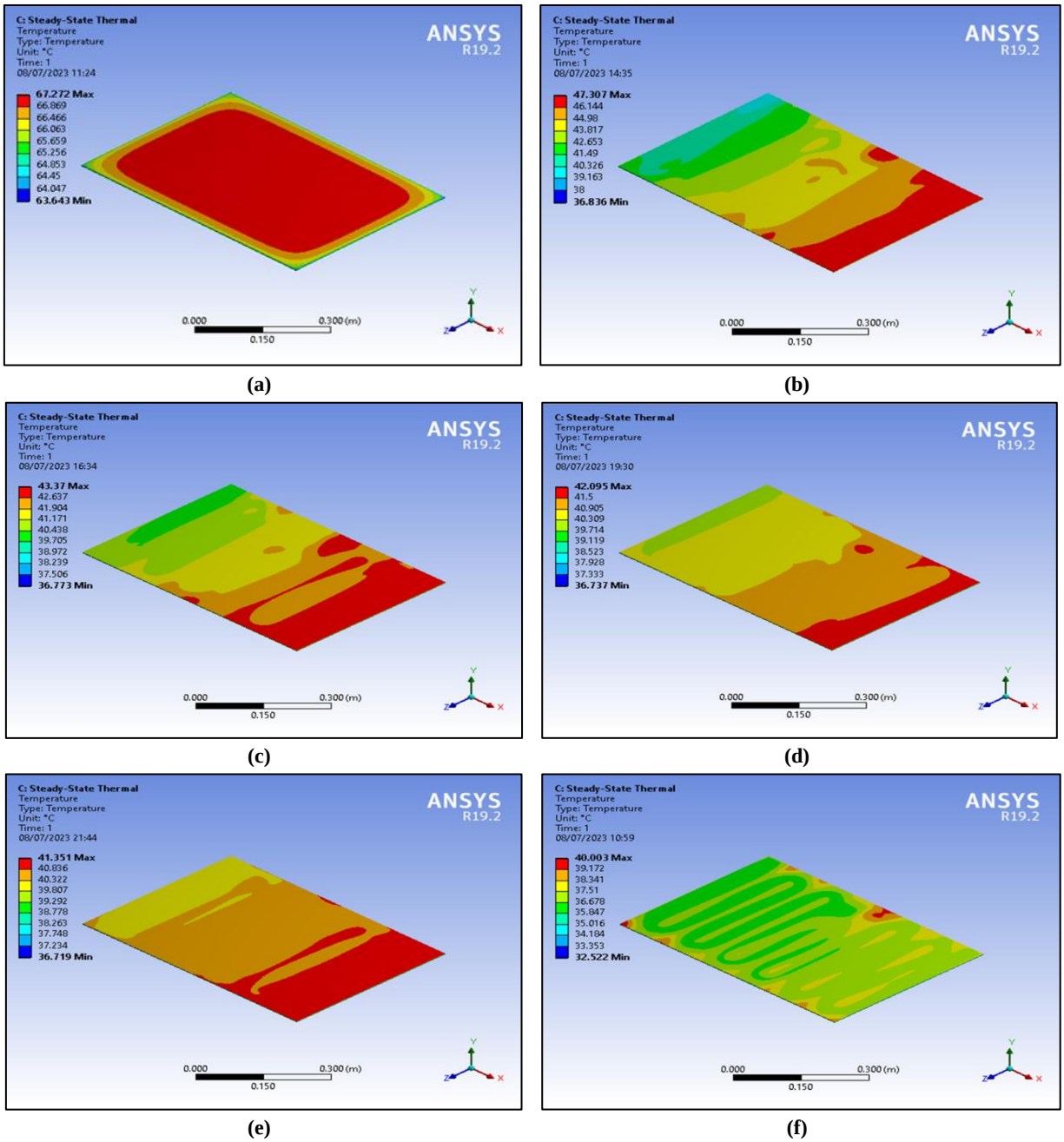

Figure 15: Effect of changing the flow rate on the temperature distribution of the surface of PV panel under solar radiation of 1035 W/m² for flow rates (a) without cooling, (b) 0.5 L/min, (c) 1L/min, (d) 2 L/min, (e) 3L/min and (f) 4L/min

4.8 Temperature distribution of cooling water through the cooling box

Figure 16 (a-f) shows the temperature distribution along the surface of the cooling water, from the inlet to the outlet. The contour plots show that the temperature distribution is more uniform in the proximal half of the outlet region, representing the heat collection area as the flow continues, especially at flow rates of 0.3, 0.5, and 1 L/min. The temperatures are staggered and less uniform for the other half of the panel near the entrance, especially the area near the middle of the cooler box. For a flow rate of 2 L/min, it is distributed almost uniformly until it reaches complete homogeneity at flow rates of 3 and 4 L/min, except for some hot spots at a flow rate of 4 L/min (the reasons for this are given in the analysis of paragraph 4.7).

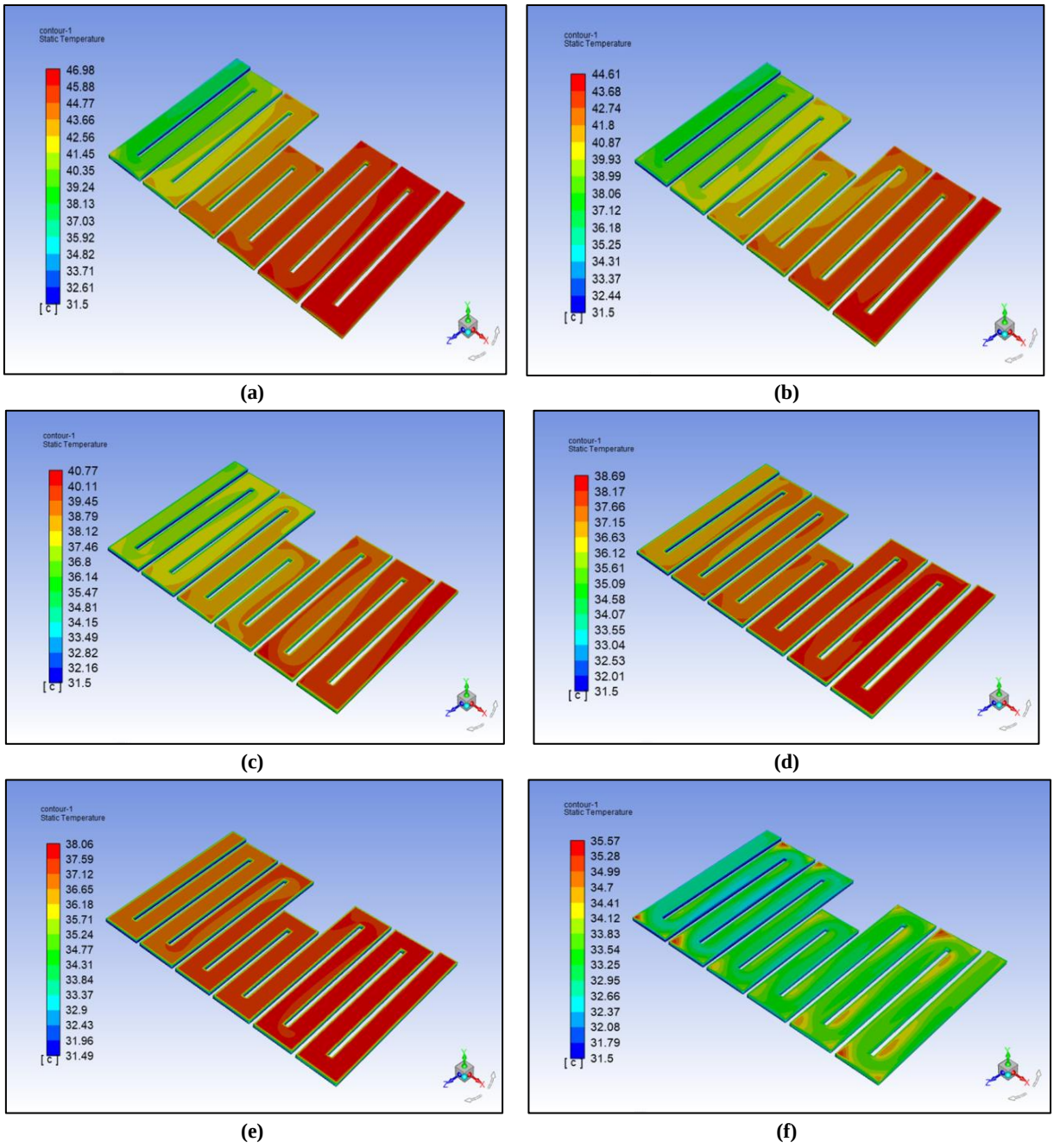

Figure 16: Effect of changing the flow rate on the temperature distribution of water passing through the cooling box under solar radiation of 1035 W/m² for flow rates (a) 0.3 L/min, (b) 0.5 L/min, (c) 1L/min, (d) 2 L/min, (e) 3L/min and (f) 4L/min

5. Conclusion

In this study, a new model for photovoltaic panel cooling systems was manufactured and tested experimentally and numerically. The results showed a good agreement between the two tests, except for some slight deviation, which amounted at worst to 6.94% and 6.4% for the average temperature of the PV panel and the water leaving the cooler box, respectively. The results also indicate that cooling the panel contributed to reducing the average temperature of the photovoltaic panel by about 21.8 ℃ compared to the traditional panel without cooling under a radiation intensity of 1035 W/m² and a flow rate of 0.3 L/min. In contrast, it decreased by an additional 8 ℃ at a flow rate of 4 L/min and under the same level of radiation intensity. This indicates the clear effect of increasing the flow rate in reducing the panel temperature. On the other hand, as a result of reducing the panel temperature, its efficiency increased to 15.37% and 14.87% at flow rates of 0.3 and 4 L/min and under radiation densities of 400 and 1035 W/m², respectively, compared to the traditional reference panel, which was around 14.44% and 12.97% under the same levels of radiation intensity above.

The introduction of the flow control system contributed to maintaining the electrical efficiency in the range of 15.36-15.37%, which is almost constant, with a high rationalization of cooling water consumption, reaching 29.28% of the amount of water required to cool the panel and maintaining a constant level of efficiency.

Author contributions

Conceptualization, H. Idan., H. Kadhom. and S. Faraj.; methodology, H. Idan.; software, H. Idan.; validation, H. Idan., H. Kadhom. and S. Faraj.; formal analysis, H. Idan.; investigation, H. Idan.; resources, H. Idan.; data curation, H. Idan.; writing—original draft preparation, H. Idan.; writing—review and editing, H. Idan.; visualization, H. Idan.; supervision, H. Idan., H. Kadhom. and S. Faraj.; project administration, H. Idan.; funding acquisition, H. Idan. All authors have read and agreed to the published version of the manuscript.

Funding

This research received no specific grant from any funding agency in the public, commercial, or not-for-profit sectors.

Data availability statement

The data supporting this study's findings are available on request from the corresponding author.

Conflicts of interest

The authors declare that there is no conflict of interest.

References

[1] C.A.F. Ramos, A.N. Alcaso, A.J.M. Cardoso, Photovoltaic-thermal (PVT) technology: Review and case study, IOP Conf. Ser.: Earth Environ. Sci., 354 (2019). https://doi.org/10.1088/1755-1315/354/1/012048

[2] M.R. Gomaa, M. Ahmed, H. Rezk, Temperature distribution modeling of PV and cooling water PV/T collectors through thin and thick cooling cross-fined channel box, Energy Rep., 8 (2022) 1144–1153. https://doi.org/10.1016/j.egyr.2021.11.061

[3] N.K. Baranwal, M.K. Singhal, Modelling and simulation of a spiral type hybrid photovoltaic thermal (PV/T) water collector using ANSYS, Adv. renew. energy technol., Springer Proceedings in Energy. Springer, Singapore. (2021) 127-139. https://doi.org/10.1007/978-981-16-0235-1_10

[4] H.A. Hussein, A.H. Numan, R.A. Abdulrahman, Improving the hybrid photovoltaic/thermal system performance using water-cooling technique and Zn-H_2O nanofluid, Hindawi Int. J. Photoenergy, (2017) 14. https://doi.org/10.1155/2017/6919054

[5] N. Kaewchoothong, T. Sukato, P. Narato, C. Nuntadusit, Flow and heat transfer characteristics on thermal performance inside the parallel flow channel with alternative ribs based on photovoltaic/thermal (PV/T) system, Applied Thermal Eng., 185 (2021) 116237. https://doi.org/10.1016/j .applthermaleng .2020.116237.

[6] J.M. Jalil, M.K. Ahmed, H.A. Idan, Experimental and numerical study of a new corrugated and packing solar collector, IOP Conf. Ser.: Mater. Sci. Eng.,765 (2020) 012026. https://doi.org/10.1088/1757-899X/765/1/012026

[7] I.A. Hasan, Enhancement the performance of PV panel by using fins as heat sink, Eng. Technol. J., 36 (2018) 798-805. https://doi.org/10.30684/etj.36.7A.13

[8] S. Saadi, S. Benissaad, S. Poncet, Y. Kabar, Effective cooling of photovoltaic solar cells by inserting triangular ribs: A numerical study, Int. J. Energy Environ. Eng., 12 (2018) 482-488.

[9] Y. Lia, F. Sun, G. Xie, J. Qin, Improved thermal performance of cooling channels with truncated ribs for a scramjet combustor fueled by endothermic hydrocarbon, Applied Thermal Eng., 142 (2018) 695-708. https://doi.org/10.1016/j.applthermaleng.2018.07.055

[10] S.M. Shalaby, M.K. Elfakharany, B.M. Moharram, H.F. Abosheiasha, Experimental study on the performance of PV with water cooling, Energy Reports., 8 (2022) 957-961. https://doi.org/10.1016/j.egyr.2021.11.155

[11] C.Y. Mah, B.H. Lim, C.W. Wong, M.H. Tan, K.K. Chong, A.C. Lai, Investigating the Performance Improvement of a Photovoltaic System in a Tropical Climate using Water Cooling Method, Energy Procedia., 159 (2019) 78-83. https://doi.org/10.1016/j.egypro.2018.12.022

[12] G. Zanlorenzi, A.L. Szejka, O.C. Junior, Hybrid photovoltaic module for efficiency improvement through an automatic water cooling system: a prototype case study, J. Clean. Prod., 196 (2018) 535-546. https://doi.org/10.1016/j.jclepro.2018.06.065

[13] K.K. Chong, W.C. Tan, Study of automotive radiator cooling system for dense-array concentration photovoltaic system, Solar Energy., 86 (2012) 2632-2643. https://doi.org/10.1016/j.solener.2012.05.033

[14] S.S.C. Ghadikolaei, Solar photovoltaic cells performance improvement by cooling technology: An overall review, 46 (2021) 10939-10972. https://doi.org/10.1016/j.ijhydene.2020.12.164

[15] S.A. Zubeer, H.A. Mohammed, M. Ilkan, A review of photovoltaic cells cooling techniques, E3S Web of Conferences., 22 (2017) 11. https://doi.org/10.1051/e3sconf/20172200205

[16] N. F. Hussein, A.A. Ismaeel, A.K. Ibrahim, Influence of detergents types and clean method on PV cells performance: An experimental study, IOP Conf. Ser.: Mater. Sci. Eng., 863 (2020). 012057 10.1088/1757-899X/863/1/012057

[17] M. A.M. Rosli, Y.J. Ping, S. Misha, M.Z. Akop, K. Sopian, S. Mat, A.N. Al-Shamani, M.A. Saruni, Simulation Study of Computational fluid dynamics on photovoltaic thermal water collector with different designs of absorber tube, J. Adv. Res. Fluid Mech. Therm. Sci., 52 (2018) 12-22.

[18] F. Bayrak, H.F. Oztop, F. Selimefendigil, Experimental study for the application of different cooling techniques in photovoltaic (PV) panels, Energy Convers. Manage., 212 (2020) 112789. https://doi.org/10.1016/j.enconman.2020.112789

[19] A. Tiwari, M.S. Sodha, Performance evaluation of solar PV/T system: an experimental validation, Sol. Energy., 80 (2006) 751–759. https://doi.org/10.1016/j.solener.2005.07.006

[20] C.G. Popovici, S.V. Hudișteanu, T.D. Mateescu, N.C. Cherecheș, Efficiency improvement of photovoltaic panels by using air cooled heat sinks, Energy Procedia., 85 (2016) 425-432. https://doi.org/10.1016/j.egypro.2015.12.223

[21] S. Sugianto, Comparative analysis of solar cell efficiency between monocrystalline and polycrystalline, INTEK J. Penelitian, 7 (2020) 92-100. http://dx.doi.org/10.31963/intek.v7i2.2625